

**SORAFENIB AND SUNITINIB, TWO ANTI-CANCER DRUGS, INHIBIT CYP3A4-  
AND ACTIVATE CYP3A5-MEDIATED MIDAZOLAM 1'-HYDROXYLATION**

Minako Sugiyama, Ken-ichi Fujita, Norie Murayama, Yuko Akiyama, Hiroshi Yamazaki, and Yasutsuna Sasaki

Department of Medical Oncology, International Medical Center-Comprehensive Cancer Center, Saitama Medical University, Hidaka 350-1298, Japan (*M.S., K.F., K.Y., Y.A., Y.S.*); Project Research Laboratory, Research Center for Genomic Medicine, Saitama Medical University, Hidaka 350-1241, Japan (*M.S., K.F., Y.A., Y.S.*); Laboratory of Drug Metabolism and Pharmacokinetics, Showa Pharmaceutical University, 3-3165 Higashi-tamagawa Gakuen, Machida, Tokyo 194-8543, Japan (*N.M., H.Y.*).

**Running title:** Cooperativity of CYP3A5 with sorafenib or sunitinib

**To whom correspondence should be addressed:**

Dr. Ken-ichi Fujita, Department of Medical Oncology, International Medical  
Center-Comprehensive Cancer Center, Saitama Medical University,  
1397-1 Yamane, Hidaka, Saitama 350-1298, Japan,  
Tel +81-42-984-4733, Fax +81-42-984-4679, E-mail fujitak@saitama-med.ac.jp

Number of text pages (until the references): 25

Number of figures: 6

Number of references: 30

Number of words in Abstract: 248

Number of words in Introduction: 627

Number of words in Discussion: 892

Abbreviations used are: CYP, individual forms of P450; FDA, the United States Food  
and Drug Administration; HLM, human liver microsomes; P450, general term for  
cytochrome P450;  $K_i$ , inhibition constant.

## Abstract

Sorafenib and sunitinib are novel small-molecule molecularly targeted anticancer drugs that inhibit multiple tyrosine kinases. These medicines have shown survival benefits in advanced renal cell carcinomas, as well as in advanced hepatocellular carcinomas and gastrointestinal stromal tumors, respectively. Effects of sorafenib and sunitinib on midazolam 1'-hydroxylation catalyzed by human CYP3A4 or CYP3A5 were investigated. Sorafenib and sunitinib inhibited metabolic reactions catalyzed by recombinant CYP3A4. Midazolam hydroxylation was also inhibited in human liver microsomes harboring the *CYP3A5\*3/\*3* genotype (poor CYP3A5 expressor). In contrast, midazolam 1'-hydroxylation catalyzed by recombinant CYP3A5 was enhanced by the coexistence of sorafenib or sunitinib in a concentration-dependent manner, with saturation occurring around 10  $\mu$ M. Midazolam hydroxylation was also enhanced in human liver microsomal samples harboring the *CYP3A5\*1/\*1* genotype (extensive CYP3A5 expressor). Sorafenib *N*-oxidation and sunitinib *N*-deethylation, the primary routes of metabolism, were predominantly catalyzed by CYP3A4, but not by CYP3A5. Preincubation period of sorafenib and sunitinib before the midazolam addition in reaction mixture did not affect the enhancement of CYP3A5-catalyzed midazolam hydroxylation, indicating that the enhancement was caused by parent sorafenib and sunitinib. Docking studies with a CYP3A5 homology model based on the structure of CYP3A4 revealed that midazolam closely docked to the heme of CYP3A5 as compared with

sorafenib or sunitinib, suggesting that these anticancer drugs act as enhancers, not as substrates. Our results thus showed that sorafenib and sunitinib activated midazolam 1'-hydroxylation by CYP3A5, but inhibited that by CYP3A4. Unexpected drug interactions involving sorafenib and sunitinib might occur via heterotropic cooperativity of CYP3A5.

## Introduction

Cytochrome P450 (P450 or CYP) is a heme-containing enzyme that catalyzes the oxidation of a wide variety of endogenous and exogenous compounds, including therapeutic drugs, carcinogens, and other xenobiotics (Nelson et al., 1996). CYP3A4, one of the major forms, is the most abundant P450 expressed in human livers (Shimada et al., 1994) as well as in small intestine (Kolars et al., 1992). CYP3A4 has been shown to participate in the metabolism of more than 30% of all therapeutic drugs or 50% of therapeutic drugs that undergo biotransformation (Lamba et al., 2002b; Matsumura et al., 2004). In adults, CYP3A5 is polymorphically expressed in approximately 10% to 40% of Caucasians, 33% of Japanese, and 50% of African Americans (Lamba et al., 2002a). The relative amount of CYP3A5 to total hepatic CYP3A protein varies, but can exceed 50% (Kuehl et al., 2001). CYP3A5 shares 84% amino-acid-sequence homology with CYP3A4. CYP3A5 and CYP3A4 overlap in their substrate specificities, but the relative importance of CYP3A5 and CYP3A4 in overall CYP3A-mediated metabolism differs between substrates (Lamba et al., 2002a; Niwa et al., 2008).

Recent progress in the development of molecularly targeted anticancer drugs has led to the approval of a variety of small-molecule tyrosine kinase inhibitors. These are orally bioavailable molecules that generally reversibly bind to intracellular ATP-binding sites of receptor(s) located inside the cell surface or to binding sites of cytoplasmic factors involved in signal transduction, thereby affecting cell

proliferation, apoptosis, or angiogenesis. Sorafenib and sunitinib (chemical structures of sorafenib in Wilhelm et al., 2004 and sunitinib in Chow and Eckhardt, 2007) are multikinase inhibitors that target various factors, such as Raf, vascular endothelial growth factor receptors 1, 2, and 3; platelet-derived growth factor receptors  $\alpha$  and  $\beta$ ; FMS-like tyrosine kinase 3; c-Kit protein; and RET receptor, affecting tumor cell proliferation and tumor angiogenesis (Wilhelm et al., 2004; Carlomagno et al., 2006; Chow and Eckhardt, 2007; Escudier et al., 2007; Llovet et al., 2008). Sorafenib is approved by the United States Food and Drug Administration (FDA) and other global health authorities for the treatment of advanced renal and hepatocellular carcinomas, because significant survival advantages were confirmed (Escudier et al., 2007; Llovet et al., 2008). Definitive efficacy of sunitinib has been demonstrated in advanced renal cell carcinoma and in imatinib-refractory gastrointestinal stromal tumors, leading to the FDA approval of sunitinib for the treatment of these diseases (Chow and Eckhardt, 2007). These multikinase inhibitors are predominantly metabolized by CYP3A4. Sorafenib is known to undergo *N*-oxidation by CYP3A4 (Lathia et al., 2006). Sunitinib *N*-deethylation, which produces a pharmacologically active metabolite, is also catalyzed by this drug-metabolizing enzyme (Rock et al., 2007). However, the roles of CYP3A5 in the metabolism of these anticancer drugs have not been reported.

Drug-drug interactions have received increasing attention over the past few decades. A recent survey indicated that approximately 30% of the United States

population older than 57-years takes at least 5 prescription drugs at any given time (Qato et al., 2008). Many drug-drug interactions involve inhibition of drug-metabolizing enzymes and transporters, resulting in increased systemic exposure and subsequent adverse drug reactions (Zhang et al., 2010). Therefore, evaluation of drug-drug interaction potential is an essential part of risk assessment to ensure the safe use of medicines, including sorafenib and sunitinib. Although information on the effects of CYP3A inhibitors on the metabolism of sorafenib or sunitinib is available (Lathia et al., 2006) (sorafenib prescribing information by the FDA, [http://www.accessdata.fda.gov/drugsatfda\\_docs/label/2007/021923s004s005s006s007lbl.pdf](http://www.accessdata.fda.gov/drugsatfda_docs/label/2007/021923s004s005s006s007lbl.pdf) and sunitinib prescribing information by the FDA, [http://www.accessdata.fda.gov/drugsatfda\\_docs/label/2010/021938s010s011s014s015lbl.pdf](http://www.accessdata.fda.gov/drugsatfda_docs/label/2010/021938s010s011s014s015lbl.pdf)), the potency of sorafenib or sunitinib for modulating CYP3A4- and CYP3A5-mediated metabolism of other therapeutic drugs has not been reported.

We thus compared the effects of sorafenib and sunitinib on midazolam 1'-hydroxylation, which is catalyzed by both CYP3A4 and CYP3A5. We also examined the contributions of CYP3A5 to sorafenib *N*-oxidation and sunitinib *N*-deethylation.

## Materials and methods

**Chemicals.** Sorafenib, sorafenib *N*-oxide, sunitinib, and *N*-desethylsunitinib were obtained from Toronto Research Chemicals (North York, Canada). Ranitidine

hydrochloride and tolnaftate were products of Sigma-Aldrich Japan (Tokyo, Japan). Midazolam hydrochloride and 1'-hydroxymidazolam were from Daiichi Pure Chemicals (Tokyo, Japan). Clonazepam was from Wako Pure Chemical Industries (Osaka, Japan). All chemicals and solvents were of the highest grade commercially available.

**Recombinant human CYP3A4 and CYP3A5, and human liver microsomes.**

Recombinant CYP3A4 and CYP3A5 co-expressed with NADPH-P450 reductase and cytochrome b<sub>5</sub> in the microsomes of insect cells with baculovirus systems were purchased from BD Biosciences (Woburn, MA). Insect microsomes were diluted in 100 mM potassium phosphate (pH 7.4). P450 contents were 1000 pmol/mL in both insect microsomal preparations.

Human liver microsomes (HLM) prepared from an African-American man (56 years) possessing *CYP3A5*\*1/\*1 and HLM from a Caucasian woman (54 years) harboring *CYP3A5*\*3/\*3 were obtained from BD Biosciences (Woburn, MA). Testosterone 6 $\beta$ -hydroxylase activities of the *CYP3A5*\*1/\*1 and *CYP3A5*\*3/\*3 HLMs as measured by BD Biosciences (Woburn, MA) were 5.8 and 13.6 nmol/min/mg protein, respectively. Expression levels of CYP3A4 and CYP3A5 as determined by Western blotting in the *CYP3A5*\*1/\*1 and *CYP3A5*\*3/\*3 HLMs were 170 and 13 pmol/mg protein, and 120 pmol/mg protein and under the detection limit, respectively. All HLMs were diluted in 250 mM sucrose. The microsomal protein content was 20 mg/mL.



**Effects of sorafenib and sunitinib on midazolam 1'-hydroxylation by CYP3A4 or CYP3A5.** Midazolam 1'-hydroxylation catalyzed by recombinant CYP3A4 or CYP3A5, or by HLM harboring CYP3A5\*1/\*1 or \*3/\*3 was tested as described elsewhere (Fujita et al., 2005). The metabolite 1'-hydroxymidazolam was quantified by the methods of Fujita et al. (Fujita et al., 2003). Effects of sorafenib and sunitinib on midazolam 1'-hydroxylation were examined as described by Fujita et al. (Fujita et al., 2005). To determine the inhibition constant ( $K_i$ ) of sorafenib or sunitinib for midazolam 1'-hydroxylation by recombinant CYP3A4, concentrations of sorafenib and sunitinib ranged from 1 to 10 and 1 to 20  $\mu$ M, respectively. Concentrations of midazolam ranging from 5 to 20  $\mu$ M were used to estimate the  $K_i$ .  $K_i$  values were calculated by nonlinear regression analysis, using the equation (1) for competitive inhibition with GraphPad Prism version 5 software (GraphPad Software, La Jolla, CA):

$$v = V_{\max} \cdot [S] / (K_m \cdot (1 + [I] / K_i) + [S]) \quad (1),$$

where  $v$ ,  $V_{\max}$ ,  $[S]$ ,  $K_m$ , and  $[I]$  are velocity, maximum velocity, substrate concentration, Michaelis constant, and inhibitor concentration, respectively.  $K_i$  is reported herein as the mean  $\pm$  standard error.

**Sorafenib N-oxidation by CYP3A4 or CYP3A5.** Sorafenib N-oxidation by recombinant CYP3A4 or CYP3A5 was examined as follows. A typical incubation mixture consisted of 100 mM sodium potassium phosphate buffer (pH 7.4), an NADPH-generating system (1.3 mM NADP<sup>+</sup>, 3.3 mM MgCl<sub>2</sub>, 3.8 mM glucose

6-phosphate, and 0.4 unit/mL glucose-6-phosphate dehydrogenase), and recombinant CYP3A4 or CYP3A5 in a final volume of 0.25 mL. The time-dependent formation of sorafenib *N*-oxide was assessed with a sorafenib concentration of 50  $\mu$ M and a CYP concentration of 20 nM. Sorafenib *N*-oxide was analyzed by a computerized Hitachi model 7000 HPLC system (Tokyo, Japan) as described previously (Afify et al., 2004) with slight modifications. Briefly, the HPLC system was equipped with a TSK-gel ODS-120T analytical column (4.6  $\times$  250 mm; 4  $\mu$ m; TOSOH, Tokyo, Japan). The metabolite was quantified by comparing the HPLC peak area to that of the internal standard tolnaftate. The lower limit of quantification of sorafenib *N*-oxide was 0.06  $\mu$ M. The intra- and inter-assay coefficient variations at 2  $\mu$ M sorafenib *N*-oxide were under 4.3% and 4.5%, respectively. Each assay was performed three times in duplicate.

**Sunitinib *N*-deethylation by CYP3A5 or CYP3A4.** Sunitinib *N*-deethylation by recombinant CYP3A4 or CYP3A5 was examined using the same methods as described for sorafenib *N*-oxidation. The time-dependent formation of *N*-desethylsunitinib was assessed at a sunitinib concentration of 200  $\mu$ M and a P450 concentration of 20 nM. *N*-desethylsunitinib was analyzed by a computerized HPLC system (Hitachi model 7000 series, Hitachi, Tokyo, Japan) as described previously (Blanchet et al., 2009) with minor modifications. Briefly, the HPLC system was equipped with a YMC-Pack CN analytical column (4.6  $\times$  250 mm; 5  $\mu$ m; YMC, Kyoto, Japan). The metabolite was quantified by comparing the HPLC peak area to that of

the internal standard ranitidine. The lower limit of quantification of *N*-desethylsunitinib was 0.25  $\mu\text{M}$ . The intra- and inter-assay coefficient variations at 0.8  $\mu\text{M}$  *N*-desethylsunitinib were under 7.9% and 7.2%, respectively. Each assay was performed three times in duplicate.

**Enzyme kinetics of sorafenib *N*-oxidation and sunitinib *N*-deethylation.** In the assays of sorafenib *N*-oxidation by recombinant CYP3A4, the CYP content and reaction time were predetermined with 50  $\mu\text{M}$  sorafenib, based on the linearity between the microsomal P450 concentration (up to 20 nM) and the reaction time (up to 5 min) versus the rate of metabolite formation. On the basis of the results, the CYP content and the reaction time were determined to be 20 nM and 5 min, respectively. The concentrations of sorafenib for enzyme kinetics ranged from 1.9 to 30  $\mu\text{M}$  for CYP3A4. In the assays of sunitinib *N*-deethylation, the protein content and the reaction time were determined to be 20 nM and 10 min, respectively, for CYP3A4 expressing microsomes and 20 nM and 20 min, respectively, for CYP3A5 expressing microsomes. The concentrations of sunitinib for enzyme kinetics ranged from 12.5 to 200  $\mu\text{M}$  for CYP3A4 and from 18.8 to 300  $\mu\text{M}$  for CYP3A5. Data points were fitted to the Michaelis-Menten equation by nonlinear least-squares regression analysis with the use of GraphPad Prism version 5 software (GraphPad Software). Kinetic constants ( $K_m$  and  $V_{max}$ ) are reported as the means  $\pm$  standard error.

**Docking simulation of sorafenib or sunitinib into reported structure of CYP3A4 and a homology model of CYP3A5.** Docking simulation was performed

as described elsewhere (Okada et al., 2009; Shimada et al., 2010). The CYP3A5 primary sequence was aligned with CYP3A4 (Protein Data Bank code 1TQN) in MOE software (version 2007.09; Chemical Computing Group, Montreal, Canada) to model a three-dimensional structure (Pearson et al., 2007). Before docking, the energy of the CYP3A4 or CYP3A5 structure was minimized by using the CHARM22 force field. Docking simulations were performed for sorafenib or sunitinib binding to the reported CYP3A4 or a homology model of CYP3A5 in the presence or absence of midazolam, using the MMFF94x force field distributed in the MOE Dock software. Twenty solutions were generated for each docking experiment and were ranked according to total interaction energy (U value).

## Results

**Modulation of midazolam 1'-hydroxylation by CYP3A4 or CYP3A5 with sorafenib or sunitinib.** As shown in Figs. 1A and 1C, sorafenib and sunitinib inhibited midazolam 1'-hydroxylation catalyzed by CYP3A4 in a dose-dependent manner. We calculated the  $K_i$  values of sorafenib and sunitinib for midazolam 1'-hydroxylation by CYP3A4. The  $K_i$  values of sorafenib and sunitinib were estimated to be  $1.7 \pm 0.3$  and  $12 \pm 0.9$   $\mu\text{M}$ , respectively. The inhibition of midazolam 1'-hydroxylation by sorafenib or sunitinib was also observed with CYP3A5-deficient HLM (CYP3A5\*3/\*3) (Fig. 2A). In contrast, midazolam 1'-hydroxylation by CYP3A5 was enhanced by the coexistence of sorafenib or sunitinib in the reaction mixture

(Fig. 1B and 1D). The enhancement was dependent on the concentration of sorafenib or sunitinib, with saturation occurring at a concentration around 10  $\mu\text{M}$ . Similar enhancement was observed with HLM (*CYP3A5\*1/\*1*) expressing CYP3A5 (Fig. 2B).  $\alpha$ -Naphthoflavone was used as positive control for the enhancement of CYP3A activity, since this chemical has been well known to show heterotropic positive cooperativity for various metabolic reactions catalyzed by CYP3A (Hutzler and Tracy, 2002). As expected,  $\alpha$ -naphthoflavone activated the midazolam 1'-hydroxylation by HLM genotyped for the *CYP3A5* gene.

**Contributions of CYP3A5 to sorafenib *N*-oxidation or sunitinib *N*-deethylation.** To address whether or not the enhancement of CYP3A5-catalyzed midazolam 1'-hydroxylation was attributed to parent sorafenib or sunitinib, we next examined the roles of CYP3A5 and CYP3A4 in sorafenib *N*-oxidation and sunitinib *N*-deethylation. The time courses of sorafenib *N*-oxidation by CYP3A4 or CYP3A5 are shown in Fig. 3A. Sorafenib *N*-oxidation by CYP3A4 was 17 times higher than that by CYP3A5 at 20 min of incubation (190 versus 11 nmol/nmol CYP). The kinetics of CYP3A4-mediated sorafenib metabolism were determined (Fig. 3C). We could not determine the kinetics of CYP3A5-mediated sorafenib metabolism, because the velocity of the reaction was not saturated by a concentration of 90  $\mu\text{M}$ . Sorafenib was not soluble in the solvent used in the present study (1% dimethyl sulfoxide) at concentrations higher than 90  $\mu\text{M}$ . The apparent  $K_m$  and  $V_{max}$  values of sorafenib *N*-oxidation by CYP3A4 were  $6.1 \pm 0.7 \mu\text{M}$ , and  $18 \pm 0.7 \text{ nmol/min/nmol}$

CYP3A4, respectively. The intrinsic metabolic clearance calculated with the  $K_m$  and  $V_{max}$  values obtained for CYP3A4 was 3.0  $\mu\text{L}/\text{min}/\text{pmol}$  CYP3A4.

The time courses of sunitinib *N*-deethylation examined with CYP3A4 or CYP3A5 are shown in Fig. 3B. Sunitinib *N*-deethylation was 3.0 times higher with CYP3A4 than with CYP3A5 at 20 min of incubation (1100 versus 370 nmol/nmol CYP3A). The kinetics of CYP3A4- or CYP3A5-mediated sunitinib metabolism were estimated (Fig. 3D). The apparent  $K_m$  and  $V_{max}$  values of sunitinib *N*-deethylation by CYP3A4 and CYP3A5 were  $32 \pm 3.3$  and  $110 \pm 12$   $\mu\text{M}$ , and  $97 \pm 3.3$  and  $35 \pm 1.7$  nmol/min/nmol CYP3A, respectively. The intrinsic metabolic clearance calculated with the  $K_m$  and  $V_{max}$  values obtained with CYP3A4 was 10 times higher than that obtained with CYP3A5 (3.0 versus 0.3  $\mu\text{L}/\text{min}/\text{pmol}$  CYP3A).

Thus, we found that sorafenib and sunitinib are substrates for CYP3A4, but not for CYP3A5. The parent compounds sorafenib and sunitinib are activators of CYP3A5-mediated midazolam 1'-hydroxylation.

**Effects of preincubation of sorafenib or sunitinib on CYP3A5-catalyzed midazolam 1'-hydroxylation.** To further test whether or not enhancement of midazolam 1'-hydroxylation by recombinant CYP3A5 was caused by parent sorafenib or sunitinib, effects of the elongation of preincubation of sorafenib or sunitinib with NADPH on midazolam 1'-hydroxylation by CYP3A5 were examined. As expected, enhancement of midazolam 1'-hydroxylation was not affected by the elongation of preincubation period (Fig. 4).

**Docking simulation of sorafenib or sunitinib into CYP3A4 and CYP3A5.** The human CYP3A4 crystal structure allowed generation of a homology model of CYP3A5, derived with the MOE program. The top-rank docking model of sorafenib or sunitinib with or without midazolam in CYP3A4 and CYP3A5 was used. Docking simulation of sorafenib or sunitinib into CYP3A4 and CYP3A5 was first performed without midazolam. Moieties in sorafenib and sunitinib, which are metabolized by CYP3A4, closely docked to the heme of CYP3A4 (Fig. 5A and 5C) with low U energy values (-36.0 and -42.6). In contrast, these moieties were found far from the heme of CYP3A5 (Fig. 5B and 5D; -25.6 and -37.2, respectively).

In the presence of midazolam, sorafenib or sunitinib molecule were also located at a similar distance from the heme of CYP3A4 (Fig. 6A and 6C) with a relatively high U energy values. In contrast, midazolam closely docked to the heme of CYP3A5 even in the presence of sorafenib or sunitinib (Fig. 6B and 6D).

## Discussion

The present study demonstrated that sorafenib and sunitinib inhibited midazolam 1'-hydroxylation catalyzed by CYP3A4, but enhanced that catalyzed by CYP3A5 (Figs 1 and 2). The enhancement of midazolam 1'-hydroxylation by CYP3A5 was most likely caused by parent sorafenib and sunitinib, not by their metabolites, because these small-molecule tyrosine kinase inhibitors were only slightly metabolized by this drug-metabolizing enzyme (Fig. 3). In addition, the

enhancement of midazolam 1'-hydroxylation was not affected by the preincubation period of either sorafenib or sunitinib with NADPH and CYP3A5 (Fig. 4). This result further supports the notion that the enhancement of midazolam 1'-hydroxylation by CYP3A5 was induced by parent sorafenib or sunitinib.

The enhancement of metabolic reactions in the presence of modulator(s), a phenomenon referred to as heterotropic cooperativity, involves two different ligands in the active site of a CYP enzyme (Hutzler and Tracy, 2002; Isin and Guengerich, 2006). Heterotropic cooperativity in CYP3A5 was recently reported by Okada et al. (Okada et al., 2009). In their study, thalidomide greatly enhanced midazolam 1'-hydroxylation and cyclosporine A oxidation by CYP3A5, consistent with our findings. These results suggest that a typical ligand universally induces heterotropic cooperativity in CYP3A5-mediated metabolism. Interestingly, however, in our other experiments using erlotinib, a small-molecule tyrosine kinase inhibitor of epidermal growth factor receptor, as a substrate of CYP3A4 and CYP3A5 (Li et al., 2007), both sorafenib and sunitinib inhibited erlotinib *O*-desmethylation (data not shown). Our results suggest that that the heterotropic cooperativity in CYP3A5-mediated metabolism associated with sorafenib or sunitinib may depend on metabolic reactions catalyzed by CYP3A5. Further studies are needed to confirm this point.

Mechanisms underlying the modulation of CYP3A4- and CYP3A5-mediated midazolam 1'-hydroxylation by sorafenib or sunitinib may be partly explained by the results of docking simulation. As shown in Fig. 6A and 6C, sorafenib or sunitinib



seemed to interfere with the binding of midazolam to the heme of CYP3A4, since these anticancer drugs and midazolam were located at similar distances from the heme of CYP3A4. These results suggest that sorafenib or sunitinib competitively inhibit CYP3A4-catalyzed midazolam 1'-hydroxylation.

In contrast, midazolam preferentially docked closely to the heme of CYP3A5, even in the coexistence of sorafenib or sunitinib (Fig. 6B and 6D). Therefore, sorafenib or sunitinib appears not to inhibit CYP3A5-mediated midazolam 1'-hydroxylation. These anticancer drugs located far from the heme may induce heterotropic cooperativity in CYP3A5-mediated metabolism, although the detailed mechanisms remain unclear.

We found that sorafenib and sunitinib were extensively metabolized by CYP3A4, but not by CYP3A5 (Fig. 3). The docking model showed that the functional groups in sorafenib and sunitinib that are metabolized by CYP3A4 docked close to the heme of the enzyme, but were located far from the heme of CYP3A5 (Fig. 5). These results supported the observations that sorafenib and sunitinib were good substrates of CYP3A4, but not of CYP3A5.

Roles of CYP3A4 and CYP3A5 in the sorafenib and sunitinib metabolisms were examined with HLM (*CYP3A5*<sup>\*1/\*1</sup>) expressing CYP3A5 and CYP3A5-deficient HLM (*CYP3A5*<sup>\*3/\*3</sup>), respectively. Sorafenib *N*-oxidation by *CYP3A5*<sup>\*1/\*1</sup> and *CYP3A5*<sup>\*3/\*3</sup> HLMs were  $0.32 \pm 0.010$  and  $0.72 \pm 0.021$  pmol/min/mg protein, respectively (n=3). Sunitinib *N*-deethylation by *CYP3A5*<sup>\*1/\*1</sup> and *CYP3A5*<sup>\*3/\*3</sup>

HLMs were  $1.6 \pm 0.027$  and  $4.9 \pm 0.16$  pmol/min/mg protein, respectively (n=3). Respective sorafenib and sunitinib concentrations were 10 and 100  $\mu$ M, and incubation period was 10 min. These results suggest that the contribution of CYP3A5 to the metabolisms of sorafenib and sunitinib might be low, which supports the results obtained with recombinant CYP3A4 and CYP3A5. However, it might be difficult to quantitatively evaluate the contributions of CYP3A4 and CYP3A5 to the metabolisms of sorafenib and sunitinib because of the reasons such as different levels of CYP3A4 expression in these microsomal preparations. Therefore, we examined the roles of CYP3A4 and CYP3A5 in the sorafenib *N*-oxidation and sunitinib *N*-deethylation with recombinant CYP3A4 and CYP3A5.

When 400 mg sorafenib was given twice daily, plasma concentration of sorafenib measured after the 14 day reached around 9  $\mu$ M (maximum and trough concentrations 10 and 8  $\mu$ M, respectively) (Minami et al., 2008). Since the activation of CYP3A5-mediated midazolam 1'-hydroxylation was observed at sorafenib concentration of 9  $\mu$ M (Fig. 1B), this medicine may activate the CYP3A5-mediated metabolism in clinical practice. In contrast, sunitinib might not affect the midazolam 1'-hydroxylation in clinical use, because the maximum plasma concentration assayed 28 days after the sunitinib treatment (50 mg/daily) was around 0.17  $\mu$ M (Shirao et al., 2010).

Considerable interpatient variability exists in the pharmacokinetics of sorafenib (Minami et al., 2008). Our present results suggest that individual variability in the

pharmacokinetics of sorafenib might be substantially associated with variable expression levels of CYP3A4, differing by more than 40 times in the liver and the small intestine, but might not be linked to genetic polymorphisms seen in CYP3A5 (Lamba et al., 2002a). In support of our hypothesis, *CYP3A5\*3* allele, which is associated with no or poor expression of functional CYP3A5 (Kuehl et al., 2001), was not significantly related to interindividual variability in the pharmacokinetics of sorafenib (Lind et al., 2010).

In conclusion, we found that sorafenib and sunitinib inhibited midazolam 1'-hydroxylation by CYP3A4, but enhanced that by CYP3A5. The present study suggests that midazolam metabolism may be increased by sorafenib and sunitinib through the heterotropic cooperativity of human CYP3A5. Because of the high frequency of polymorphic CYP3A5 expression in Asians and Africans, a relatively high frequency of unexpected drug interactions involving sorafenib (and sunitinib) might occur via CYP3A5 contribution in drug metabolism.

#### **Authorship contributions**

Participated in research design: Fujita and Sugiyama.

Conducted experiments: Sugiyama and Akiyama.

Performed data analysis: Sugiyama and Fujita.

Wrote or contributed to the writing of the manuscript: Sugiyama, Fujita and Yamazaki.

DMD #37853

Other: Murayama and Yamazaki performed docking simulation of sorafenib and sunitinib, and Sasaki acquired funding for the research.

## References

- Afify S, Rapp UR, and Hogger P (2004) Validation of a liquid chromatography assay for the quantification of the Raf kinase inhibitor BAY 43-9006 in small volumes of mouse serum. *J Chromatogr B Analyt Technol Biomed Life Sci* **809**: 99-103.
- Blanchet B, Saboureau C, Benichou AS, Billemont B, Taieb F, Ropert S, Dauphin A, Goldwasser F, and Tod M (2009) Development and validation of an HPLC-UV-visible method for sunitinib quantification in human plasma. *Clin Chim Acta* **404**: 134-139.
- Carlomagno F, Anaganti S, Guida T, Salvatore G, Troncone G, Wilhelm SM, and Santoro M (2006) BAY 43-9006 inhibition of oncogenic RET mutants. *J Natl Cancer Inst* **98**: 326-334.
- Chow LQ, and Eckhardt SG (2007) Sunitinib: from rational design to clinical efficacy. *J Clin Oncol* **25**: 884-896.
- Escudier B, Eisen T, Stadler WM, Szczylik C, Oudard S, Siebels M, Negrier S, Chevreau C, Solska E, Desai AA, Rolland F, Demkow T, Hutson TE, Gore M, Freeman S, Schwartz B, Shan M, Simantov R, Bukowski RM, and Group TS (2007) Sorafenib in advanced clear-cell renal-cell carcinoma. *N Engl J Med* **356**: 125-134.
- Fujita K, Ando Y, Narabayashi M, Miya T, Nagashima F, Yamamoto W, Kodama K, Araki K, Endo H, and Sasaki Y (2005) Gefitinib (Iressa) inhibits the CYP3A4-mediated formation of 7-ethyl-10-(4-amino-1-piperidino)carbonyloxycamptothecin but activates that of 7-ethyl-10-[4-N-(5-aminopentanoic acid)-1-piperidino]carbonyloxycamptothecin from irinotecan. *Drug Metab*

*Dispos* **33**: 1785-1790.

Fujita K, Hidaka M, Takamura N, Yamasaki K, Iwakiri T, Okumura M, Kodama H, Yamaguchi M, Ikenoue T, and Arimori K (2003) Inhibitory effects of citrus fruits on cytochrome P450 3A (CYP3A) activity in humans. *Biol Pharm Bull* **26**: 1371-1373.

Hutzler JM, and Tracy TS (2002) Atypical kinetic profiles in drug metabolism reactions. *Drug Metab Dispos* **30**: 355-362.

Isin EM, and Guengerich FP (2006) Kinetics and thermodynamics of ligand binding by cytochrome P450 3A4. *J Biol Chem* **281**: 9127-9136.

Kolars JC, Schmiedlin-Ren P, Schuetz JD, Fang C, and Watkins PB (1992) Identification of rifampin-inducible P450III<sub>A4</sub> (CYP3A<sub>4</sub>) in human small bowel enterocytes. *J Clin Invest* **90**: 1871-1878.

Kuehl P, Zhang J, Lin Y, Lamba J, Assem M, Schuetz J, Watkins PB, Daly A, Wrighton SA, Hall SD, Maurel P, Relling M, Brimer C, Yasuda K, Venkataramanan R, Strom S, Thummel K, Boguski MS, and Schuetz E (2001) Sequence diversity in CYP3A promoters and characterization of the genetic basis of polymorphic CYP3A5 expression. *Nat Genet* **27**: 383-391.

Lamba JK, Lin YS, Schuetz EG, and Thummel KE (2002a) Genetic contribution to variable human CYP3A-mediated metabolism. *Adv Drug Deliv Rev* **54**: 1271-1294.

Lamba JK, Lin YS, Thummel K, Daly A, Watkins PB, Strom S, Zhang J, and Schuetz EG (2002b) Common allelic variants of cytochrome P4503A<sub>4</sub> and their prevalence in different populations. *Pharmacogenetics* **12**: 121-132.

Lathia C, Lettieri J, Cihon F, Gallentine M, Radtke M, and Sundaresan P (2006) Lack of effect of ketoconazole-mediated CYP3A inhibition on sorafenib

- clinical pharmacokinetics. *Cancer Chemother Pharmacol* **57**: 685-692.
- Li J, Zhao M, He P, Hidalgo M, and Baker SD (2007) Differential metabolism of gefitinib and erlotinib by human cytochrome P450 enzymes. *Clin Cancer Res* **13**: 3731-3737.
- Lind JS, Dingemans AM, Groen HJ, Thunnissen FB, Bekers O, Heideman DA, Honeywell RJ, Giovannetti E, Peters GJ, Postmus PE, van Suylen RJ, and Smit EF (2010) A multicenter phase II study of erlotinib and sorafenib in chemotherapy-naive patients with advanced non-small cell lung cancer. *Clin Cancer Res* **16**: 3078-3087.
- Llovet JM, Ricci S, Mazzaferro V, Hilgard P, Gane E, Blanc JF, de Oliveira AC, Santoro A, Raoul JL, Forner A, Schwartz M, Porta C, Zeuzem S, Bolondi L, Greten TF, Galle PR, Seitz JF, Borbath I, Haussinger D, Giannaris T, Shan M, Moscovici M, Voliotis D, Bruix J, and Group SIS (2008) Sorafenib in advanced hepatocellular carcinoma. *N Engl J Med* **359**: 378-390.
- Matsumura K, Saito T, Takahashi Y, Ozeki T, Kiyotani K, Fujieda M, Yamazaki H, Kunitoh H, and Kamataki T (2004) Identification of a novel polymorphic enhancer of the human CYP3A4 gene. *Mol Pharmacol* **65**: 326-334.
- Minami H, Kawada K, Ebi H, Kitagawa K, Kim YI, Araki K, Mukai H, Tahara M, Nakajima H, and Nakajima K (2008) Phase I and pharmacokinetic study of sorafenib, an oral multikinase inhibitor, in Japanese patients with advanced refractory solid tumors. *Cancer Sci* **99**: 1492-1498.
- Nelson DR, Koymans L, Kamataki T, Stegeman JJ, Feyereisen R, Waxman DJ, Waterman MR, Gotoh O, Coon MJ, Estabrook RW, Gunsalus IC, and Nebert DW (1996) P450 superfamily: update on new sequences, gene mapping, accession numbers and nomenclature. *Pharmacogenetics* **6**: 1-42.

- Niwa T, Murayama N, Emoto C, and Yamazaki H (2008) Comparison of kinetic parameters for drug oxidation rates and substrate inhibition potential mediated by cytochrome P450 3A4 and 3A5. *Curr Drug Metab* **9**: 20-33.
- Okada Y, Murayama N, Yanagida C, Shimizu M, Guengerich FP, and Yamazaki H (2009) Drug interactions of thalidomide with midazolam and cyclosporine A: heterotropic cooperativity of human cytochrome P450 3A5. *Drug Metab Dispos* **37**: 18-23.
- Pearson JT, Wahlstrom JL, Dickmann LJ, Kumar S, Halpert JR, Wienkers LC, Foti RS, and Rock DA (2007) Differential time-dependent inactivation of P450 3A4 and P450 3A5 by raloxifene: a key role for C239 in quenching reactive intermediates. *Chem Res Toxicol* **20**: 1778-1786.
- Qato DM, Alexander GC, Conti RM, Johnson M, Schumm P, and Lindau ST (2008) Use of prescription and over-the-counter medications and dietary supplements among older adults in the United States. *JAMA* **300**: 2867-2878.
- Rock EP, Goodman V, Jiang JX, Mahjoob K, Verbois SL, Morse D, Dagher R, Justice R, and Pazdur R (2007) Food and Drug Administration drug approval summary: Sunitinib malate for the treatment of gastrointestinal stromal tumor and advanced renal cell carcinoma. *Oncologist* **12**: 107-113.
- Shimada T, Tanaka K, Takenaka S, Murayama N, Martin MV, Foroozesh MK, Yamazaki H, Guengerich FP, and Komori M (2010) Structure-Function Relationships of Inhibition of Human Cytochromes P450 1A1, 1A2, 1B1, 2C9, and 3A4 by 33 Flavonoid Derivatives. *Chem Res Toxicol*.
- Shimada T, Yamazaki H, Mimura M, Inui Y, and Guengerich FP (1994) Interindividual variations in human liver cytochrome P-450 enzymes involved



in the oxidation of drugs, carcinogens and toxic chemicals: studies with liver microsomes of 30 Japanese and 30 Caucasians. *J Pharmacol Exp Ther* **270**: 414-423.

Shirao K, Nishida T, Doi T, Komatsu Y, Muro K, Li Y, Ueda E, and Ohtsu A (2010) Phase I/II study of sunitinib malate in Japanese patients with gastrointestinal stromal tumor after failure of prior treatment with imatinib mesylate. *Invest New Drugs* **28**: 866-875.

Wilhelm SM, Carter C, Tang L, Wilkie D, McNabola A, Rong H, Chen C, Zhang X, Vincent P, McHugh M, Cao Y, Shujath J, Gawlak S, Eveleigh D, Rowley B, Liu L, Adnane L, Lynch M, Auclair D, Taylor I, Gedrich R, Voznesensky A, Riedl B, Post LE, Bollag G, and Trail PA (2004) BAY 43-9006 exhibits broad spectrum oral antitumor activity and targets the RAF/MEK/ERK pathway and receptor tyrosine kinases involved in tumor progression and angiogenesis. *Cancer Res* **64**: 7099-7109.

Zhang L, Reynolds KS, Zhao P, and Huang SM (2010) Drug interactions evaluation: an integrated part of risk assessment of therapeutics. *Toxicol Appl Pharmacol* **243**: 134-145.

### Footnotes

This study was supported in part by the Grant-in-Aid for Cancer Research 21S-8-1 from the Ministry of Health, Labour and Welfare of Japan, in part by a grant-in-aid for “Support Project of Strategic Research Center in Private Universities” from the Ministry of Education, Culture, Sports, Science and Technology (MEXT) to Saitama Medical University Research Center for Genomic Medicine, and by a Grant-in-Aid for High Technology Research Centre Project (19-8) from the MEXT of Japan to Showa Pharmaceutical University.

Reprint requests: Dr. Ken-ichi Fujita, Department of Medical Oncology, International Medical Center-Comprehensive Cancer Center, Saitama Medical University, 1397-1 Yamane, Hidaka, Saitama, 350-1298, Japan, Tel +81-42-984-4733, Fax +81-42-984-4679, E-mail [fujitak@saitama-med.ac.jp](mailto:fujitak@saitama-med.ac.jp)

## Legends for figures

**Fig. 1.** Modulation of midazolam 1'-hydroxylation activities catalyzed by CYP3A4 (A,C, open symbols) or CYP3A5 (B,D, closed symbols) in the presence of sorafenib (A,B) or sunitinib (C,D).

Midazolam 1'-hydroxylation activities were determined at substrate concentrations of 5 (○,●), 10 (△,▲), and 20 (□,■) μM, respectively. Each point shows the mean of three independent analyses with standard deviation.

**Fig. 2.** Effects of sorafenib and sunitinib on midazolam 1'-hydroxylation by human liver microsomes genotyped for *CYP3A5*\*3/\*3 (A) or *CYP3A5*\*1/\*1 (B).

Midazolam concentration used was 10 μM. Each data point shows the mean of triplicate determinations with standard deviation bars.

**Fig. 3.** Sorafenib *N*-oxidation and sunitinib *N*-deethylation activities catalyzed by CYP3A4 (A,C) or CYP3A5 (B,D).

Time courses of sorafenib *N*-oxidation (A) and sunitinib *N*-deethylation (B) by CYP3A4 (◇) or CYP3A5 (▲) and effects of substrate concentrations on sorafenib *N*-oxidation (C) and sunitinib *N*-deethylation (D) activities by CYP3A4 (◇) or CYP3A5 (▲) are shown. Each data point represents the mean of triplicate determinations and is shown with standard deviation bars.

**Fig. 4.** Effects of preincubation period with 10  $\mu\text{M}$  of sorafenib (●) or 20  $\mu\text{M}$  of sunitinib (■) in the presence of NADPH on recombinant CYP3A5-mediated midazolam hydroxylation activities at a substrate concentration of 10  $\mu\text{M}$ .

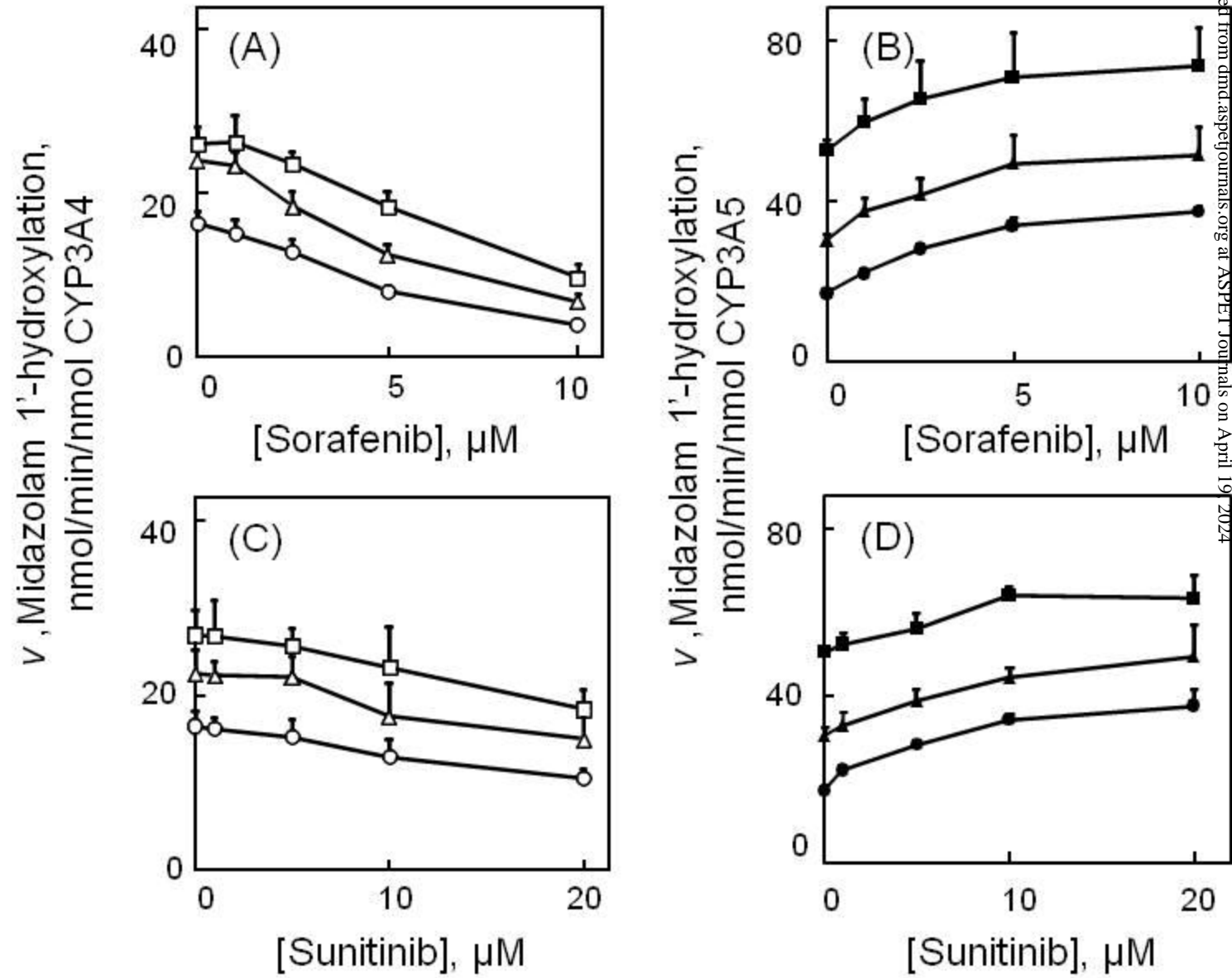
**Fig. 5.** Docking simulation of sorafenib (A,B) or sunitinib (C,D) into CYP3A4 (A,C) and CYP3A5 (B,D) in the absence of midazolam.

Drug-P450 interaction energies calculated in Figs. 4A-4D (U, kcal/mol) were -36.0, -25.6, -42.6, and -37.2, respectively. In the figure, oxygen, nitrogen, fluoride, and iron atoms are colored with red, blue, green, and light blue, respectively.

**Fig. 6.** Docking simulation of sorafenib (A,B) or sunitinib (C,D) into CYP3A4 (A,C) and CYP3A5 (B,D) in the presence of midazolam.

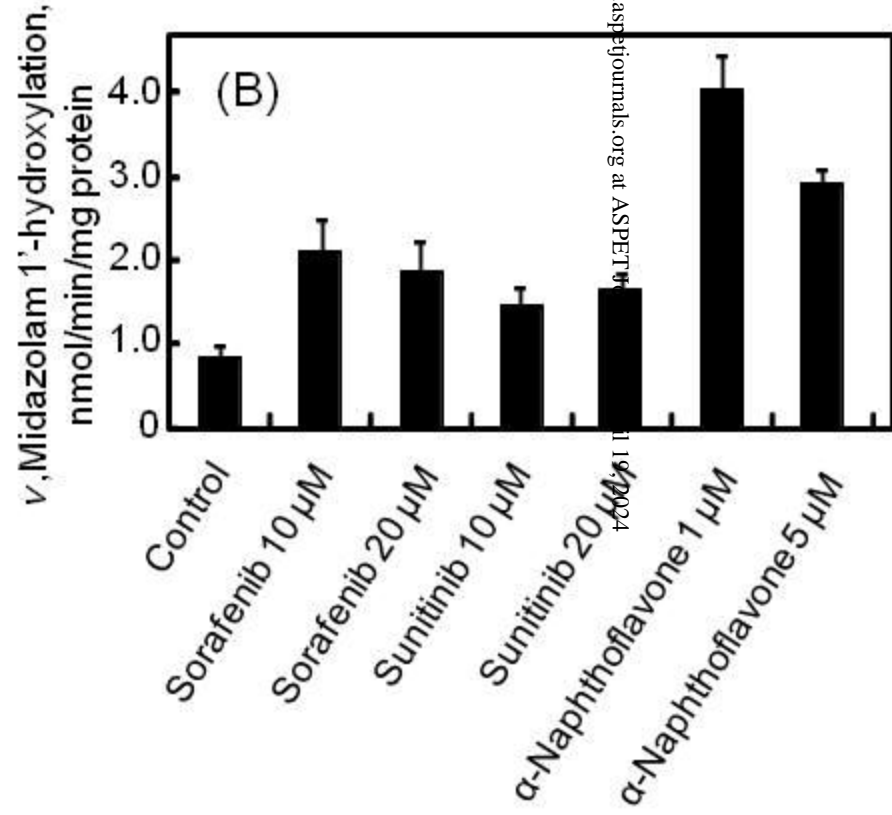
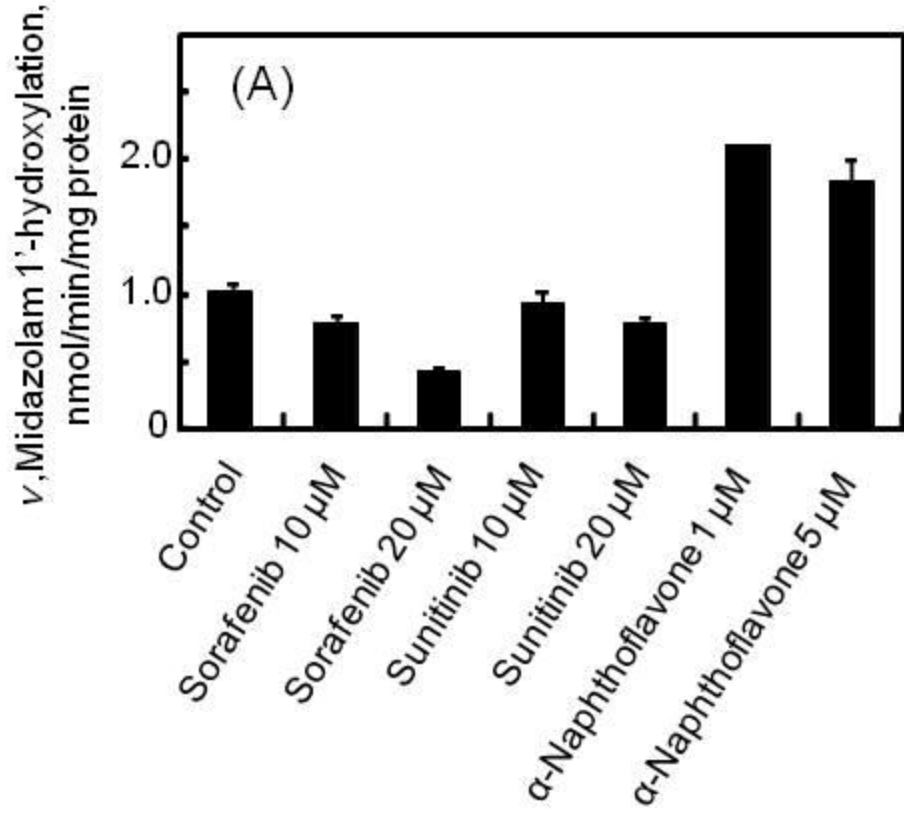
Drug-P450 interaction energies calculated in Figs. 5A-5D (U, kcal/mol) were 77.2, 259, 276, and 360, respectively. Other details are as in Figure 4.

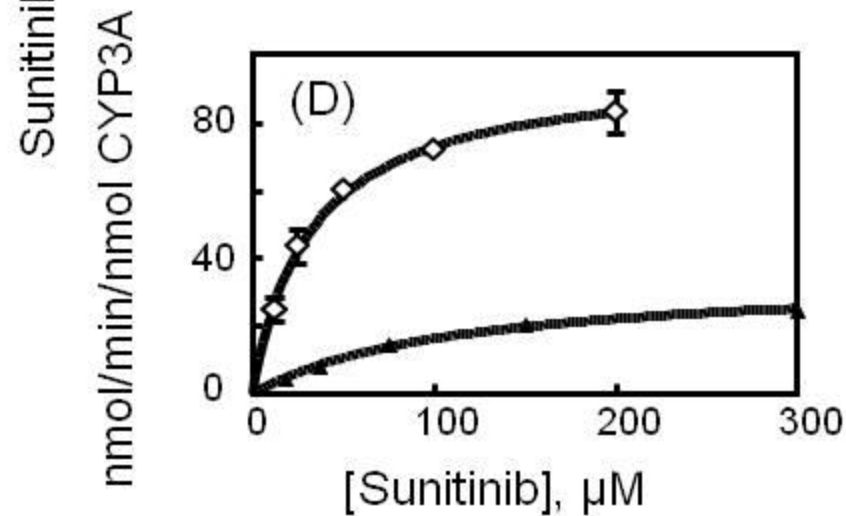
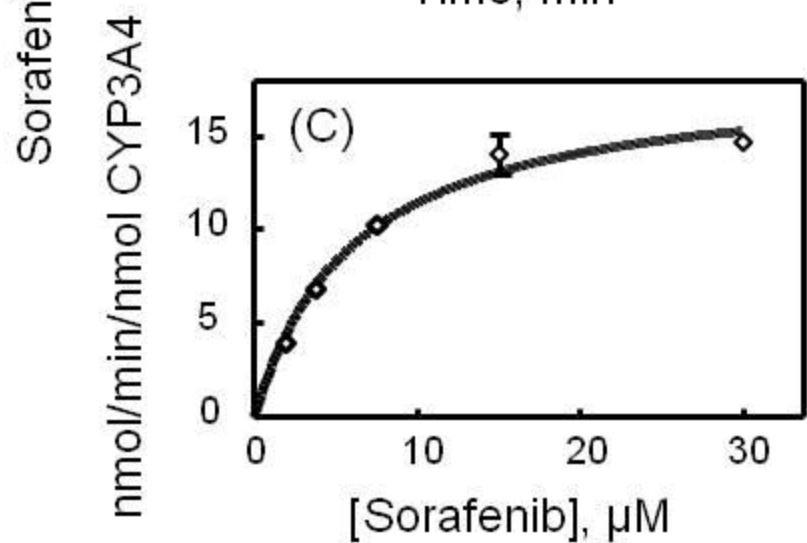
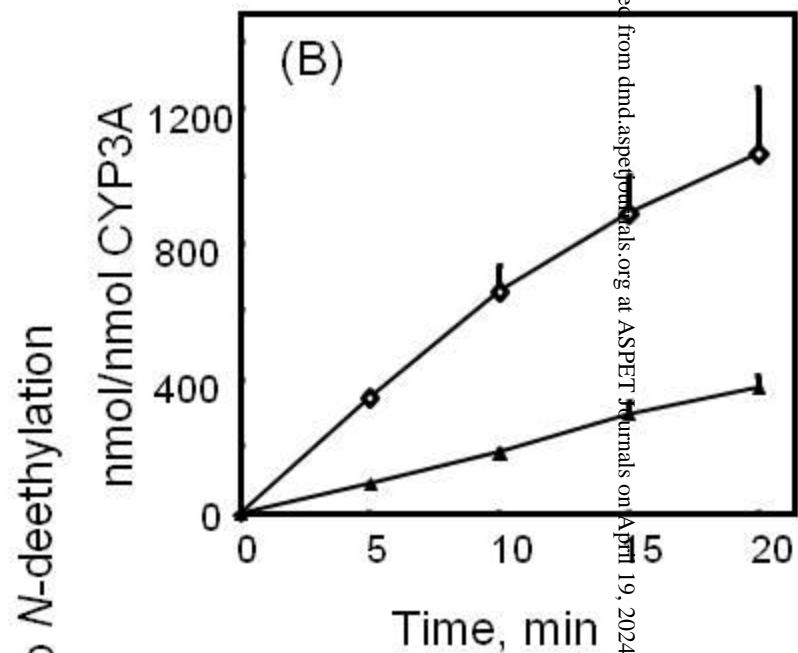
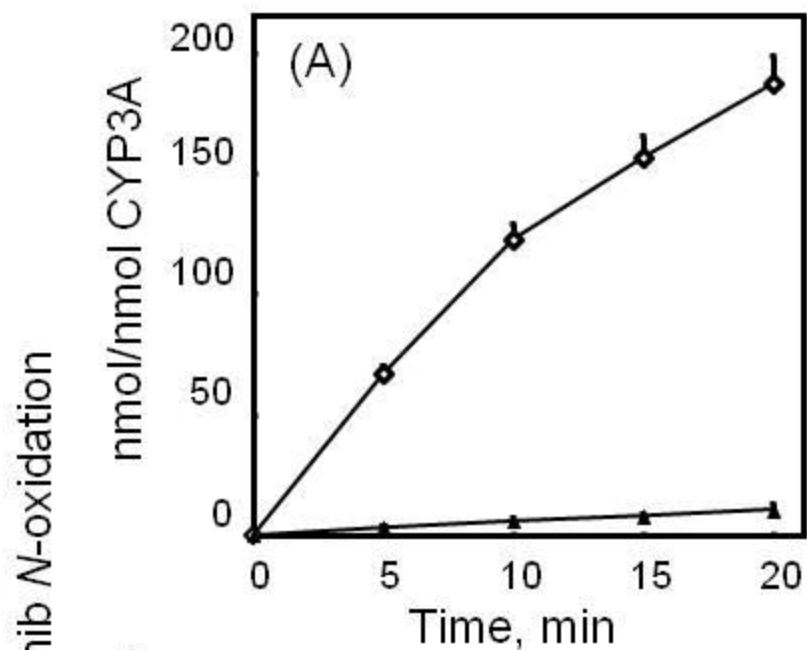
Fig. 1



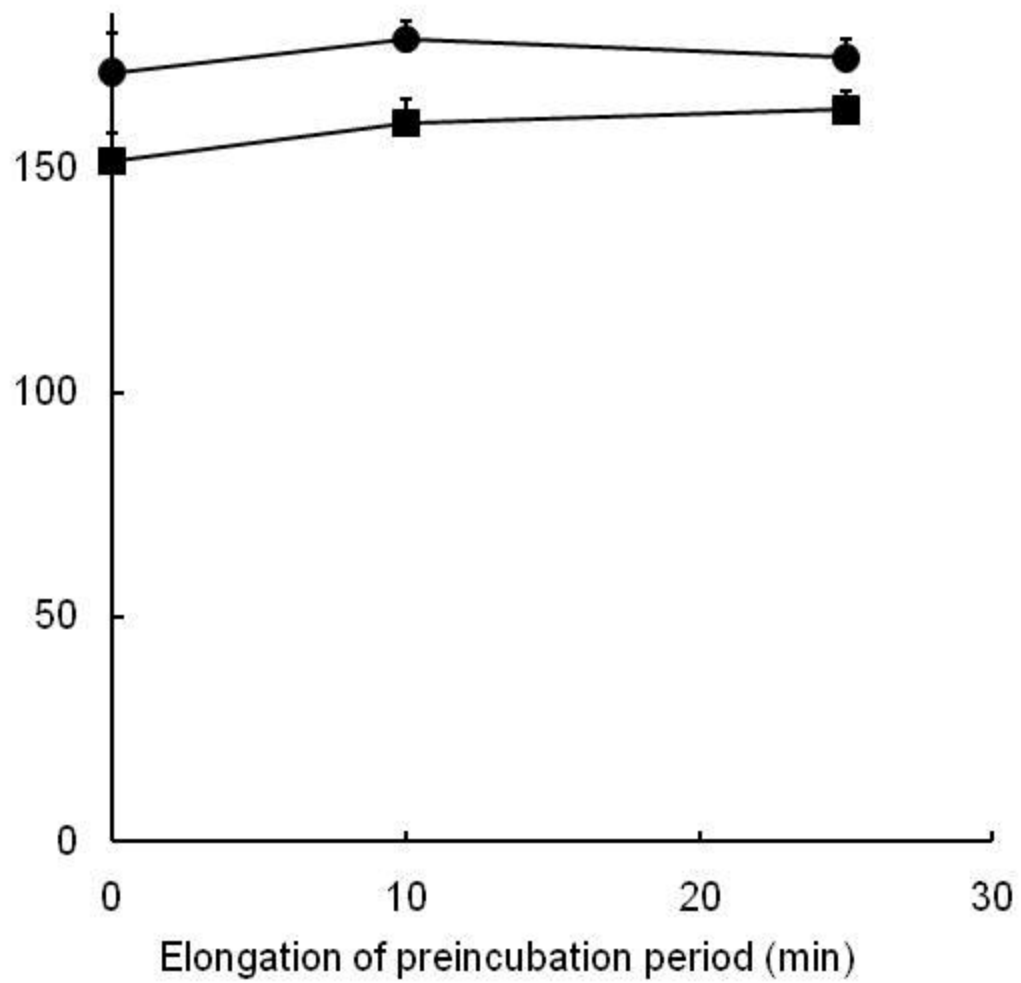
Downloaded from dmnd.aspetjournals.org at ASPET Journals on April 19, 2024

Fig. 2

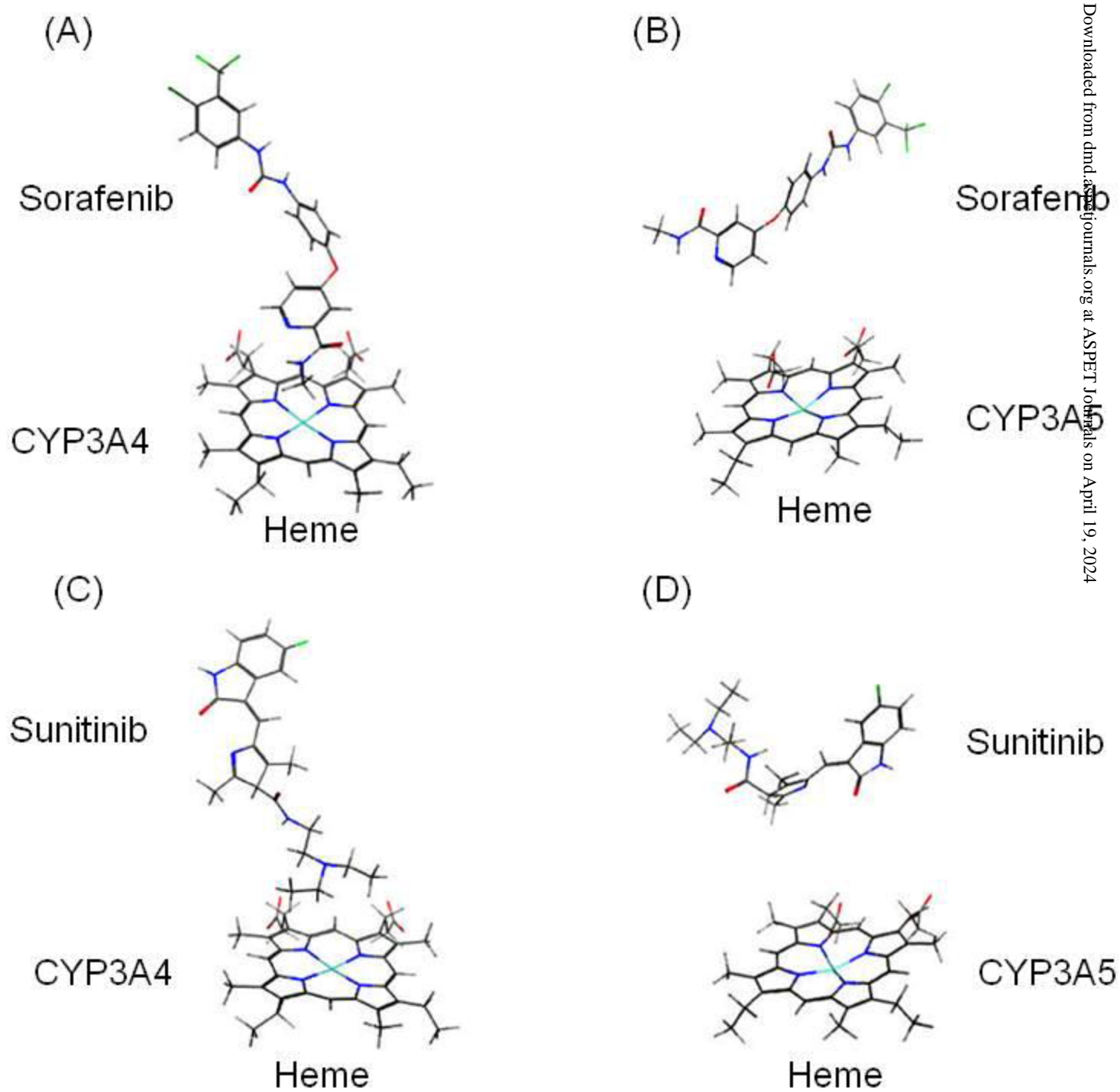


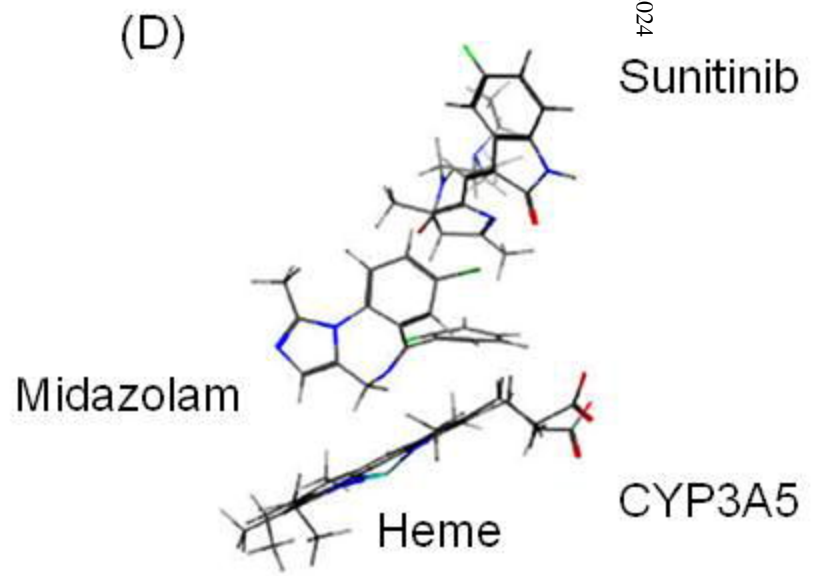
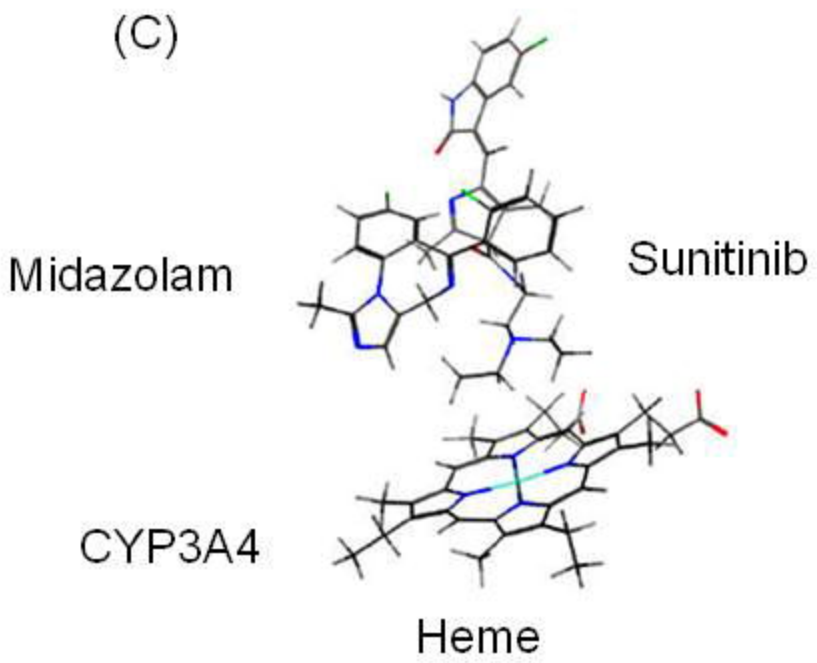
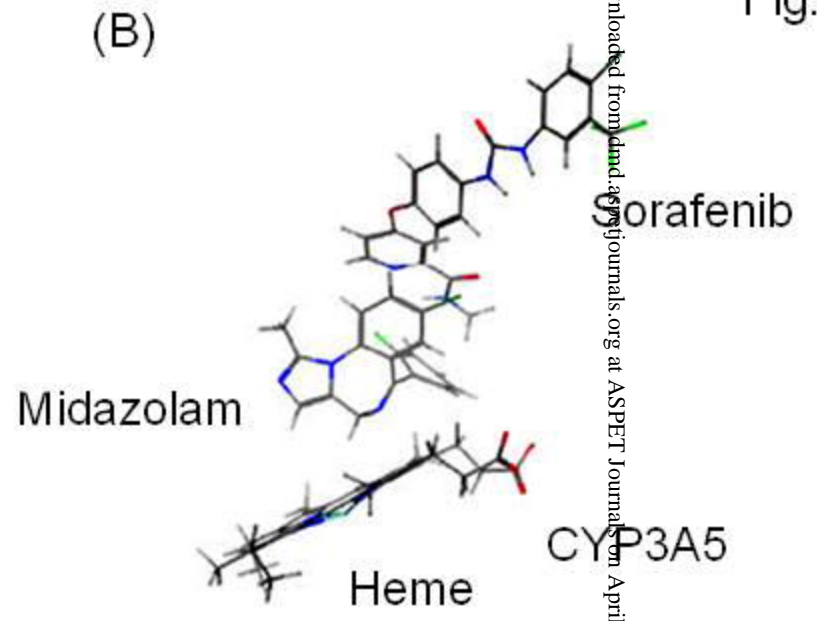
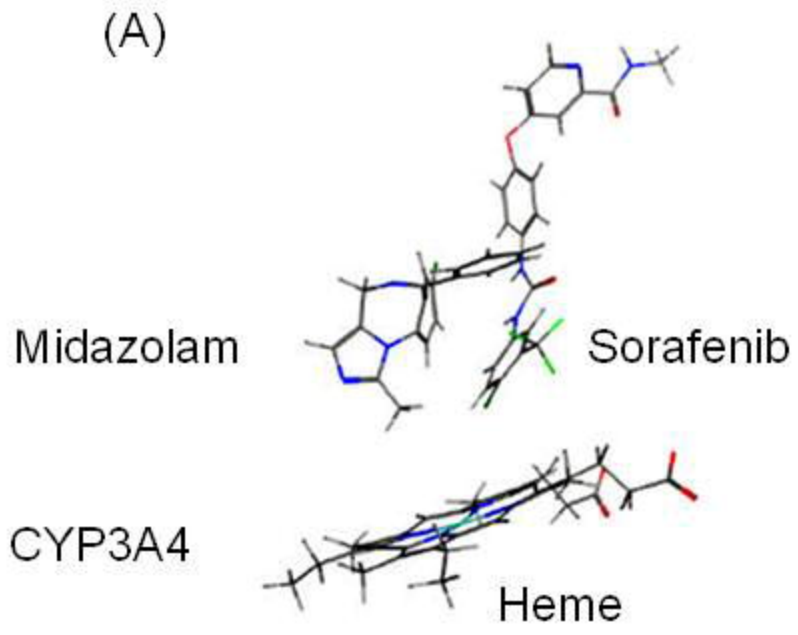


Midazolam 1'-hydroxylation by CYP3A5  
(% of control)









Downloaded from <https://pubs.aspetjournals.org/> at ASPET Journals on April 19, 2024